Synthesis and Ring-opening Metathesis Polymerization of a Strained trans-Silacycloheptene and Single Molecule Mechanics of its Polymer

Herbert Wakefield IV,[1] Ilia Kevlishvili,[2] Kelsie E. Wentz,[1] Yunxin Yao,[3] Tatiana B. Kouznetsova,[3] Sophia J. Melvin,[1] Em G. Ambrosius,[1] Abraham Herzog-Arbeitman,[4] Maxime A. Siegler,[1] Jeremiah A. Johnson,[4] Stephen L. Craig,[3] Heather J. Kulik,[2,4] Rebekka S. Klausen[1]*

Affiliations

[1] Department of Chemistry, Johns Hopkins University, Baltimore, MD, 21218, USA
[2] Department of Chemical Engineering, Massachusetts Institute of Technology, Cambridge, MA, 02139, USA
[3] Department of Chemistry, Duke University, Durham, NC, 27708, USA
[4] Department of Chemistry, Massachusetts Institute of Technology, Cambridge, MA, 02139, USA

*Correspondence to: klausen@jhu.edu

Abstract

The *cis*- and *trans*-isomers of a silacycloheptene were selectively synthesized by the alkylation of a silyl dianion, a novel approach to strained cycloalkenes. The *trans*-silacycloheptene (*trans*-SiCH) was significantly more strained than the *cis* isomer, as predicted by quantum chemical calculations and confirmed by crystallographic signatures of a twisted alkene. Each isomer exhibited distinct reactivity towards ring-opening metathesis polymerization (ROMP), where only *trans*-SiCH afforded high molar mass polymer under enthalpy-driven ROMP. Hypothesizing that the introduction of silicon might result in increased molecular compliance at large extensions, we compared poly(*trans*-SiCH) to organic polymers by single-molecule force spectroscopy (SMFS). Force-extension curves from SMFS showed that poly(*trans*-SiCH) is more easily overstretched than two carbon-based analogs, polycyclooctene and polybutadiene, with stretching constants that agree well with the results of computational simulations.

Introduction

Herein we report the geometrically selective synthesis of *trans*- and *cis*-silacycloheptenes via a novel synthetic strategy and probe the effect of Si for C substitution on ring-opening metathesis polymerization (ROMP, Figure 1a). The efficiency of ROMP, and the reverse depolymerization, is exquisitely sensitive to monomer structure. High ring strain monomers (e.g., >10 kcal mol^{-1}), as exemplified by norbornene, dicyclopentadiene, and cyclobutene rapidly polymerize in an enthalpically driven process. However, in the simple small-rings *cis*-cyclopentene to *cis*-cyclooctene, only *cis*-cyclooctene (cis-CO) is high-strain (Figure 1b). The low strain monomers *cis*-cyclopentene[1] and *cis*-cycloheptene (*cis*-CH)[2] polymerize under entropy-driven ROMP conditions, including high concentration and higher temperatures.[3,4]

While small to medium size *trans*-cycloalkenes are more strained than their *cis*-isomers,[5] investigation of *trans*-cycloalkene monomers for ROMP is limited to *trans*-CO as smaller rings are thermally unstable; e.g., *trans*-CH isomerizes to *cis*-CH at –40 °C.[6] *trans*-Cycloalkenes can be synthetically challenging, as they are typically synthesized by photoisomerization of the *cis* isomer[7,8] and the maximum yield of the *trans* isomer is limited by the photostationary state.[9] Nonetheless, *cis*- and *trans*-CO exhibit several interesting differences in ROMP reactivity. Grubbs reported that *trans*-CO undergoes living ROMP,[10] in contrast to the lower strain *cis*-CO where secondary metathesis (e.g., chain transfer) reactions eroded molecular weight control. Interconversion of *cis* and *trans*-cycloalkenes can also facilitate chemical recycling. Recently, Wang et al. demonstrated closed loop chemical recycling of bicyclic monomers containing

cyclooctene rings:[11] *trans* isomers (prepared by photoisomerization of the *cis* isomer) underwent rapid ROMP, while the linear polymer could be depolymerized to the low-strain *cis* monomer.[12]

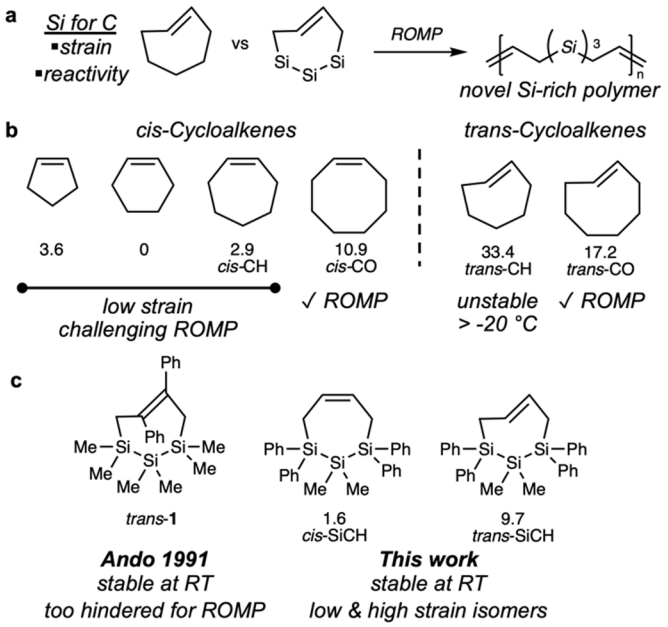

Figure 1. a) Si for C Substitution: impact on monomer ring strain and reactivity. b) Ring strain in typical *Z*- and *E*-cycloalkenes. c) Sila-cycloheptenes for ring-opening metathesis polymerization (ROMP).

Due to the longer C–Si bond, substitution of at least one carbon atom in *trans*-CH with a silicon atom partially alleviates ring strain and results in room temperature stable *trans*-cycloalkenes, as first reported by Ando in 1991,[13] and further developed by Woerpel,[14] Fox,[15] and others.[16] Thus, the Si's size and distinctive properties has implications for both the ability to generate Si-containing macrocycles and their subsequent polymerization.

At the same time, we recognized that oligosilanes of the general formula Si_nR_{2n+2} possess more low energy conformations with lower barriers to interconversion than alkanes[17,18] and that introduction of a conformationally flexible oligosilane into a macromolecule could result in striking differences in the force-coupled extensional behavior of the macromolecules relative to all-carbon congeners. Single-molecule force spectroscopy (SMFS) implemented via an atomic force microscope is a quantitative probe of the elasticity of single polymer chains, as well as intra-strand conformational change.[19–26] We hypothesized that SMFS could facilitate comparison of all carbon backbones to a Si-enriched polymer strand.

For these reasons, we became interested in the ROMP reactivity of cycloalkenes containing oligosilyl fragments, as well as the potential for ROMP to achieve novel Si-rich polymers of sufficiently high molar mass (>50 kg mol^{-1}) for macromolecular characterization by SMFS (Figure 1a). Other approaches to polysilanes, e.g., dehydrocoupling polymerization or Wurtz polymerization, suffer from low molar mass or poor control of dispersity.[27–29] While silicon-containing rings and dienes have been investigated for ROMP and acyclic diene metathesis (ADMET),[30] the silicon functional groups investigated have focused on siloxane,[31,32] silyl ether,[33–35] and acylsilane[36] containing alkenes. Oligosilanes, compromising consecutive Si–Si bonds, have not previously been investigated in ROMP or ADMET. The Si–Si bond is sensitive to cleavage by late transition metals (e.g., Rh, Pd, Pt),[37,38] which may contribute to the lack of prior investigation of oligosilyl monomers.

Herein, we report the synthesis of a room-temperature stable and ROMP-reactive *trans*-silacycloheptene (*trans*-SiCH, Figure 1c). The isomeric *cis*-silacycloheptene (*cis*-SiCH) is low strain and does not readily undergo enthalpy-driven ROMP. Control experiments and spectroscopic characterization are consistent with the stability of the oligosilyl chain to Ru-metathesis catalysts. The poly(*trans*-SiCH) is a novel example of a silicon-rich polymer, distinct from polysilanes (Si–Si), polysiloxanes (Si–O–Si), polysilazanes (Si–N–Si), and polycarbosilanes (Si–C–Si),[39–42] and of sufficiently high molar mass for SMFS characterization of single molecule mechanics.

Results & Discussion

Silacycloheptene synthesis. While Ando's silacycloheptene *trans*-**1** is stable to thermal isomerization at room temperature, the synthesis reveals representative challenges in the preparation of *trans*-cycloalkenes for ROMP (Scheme 1a). The synthesis of *trans*-**1** was low-yielding: reductive coupling of 2,3-diphenylbutadiene and 1,3-dichlorohexamethyltrisilane provided *cis*-**1** (23% yield), which was photoisomerized (254 nm) in benzene-d_6 to *trans*-**1** (19% yield), with a photostationary state close to 1:1 E:Z.[13] The tetrasubstituted stilbene is too sterically hindered for ROMP, but conjugation with aromatic rings[43] is likely necessary for selective alkene excitation relative to the trisilane chromophore.[44]

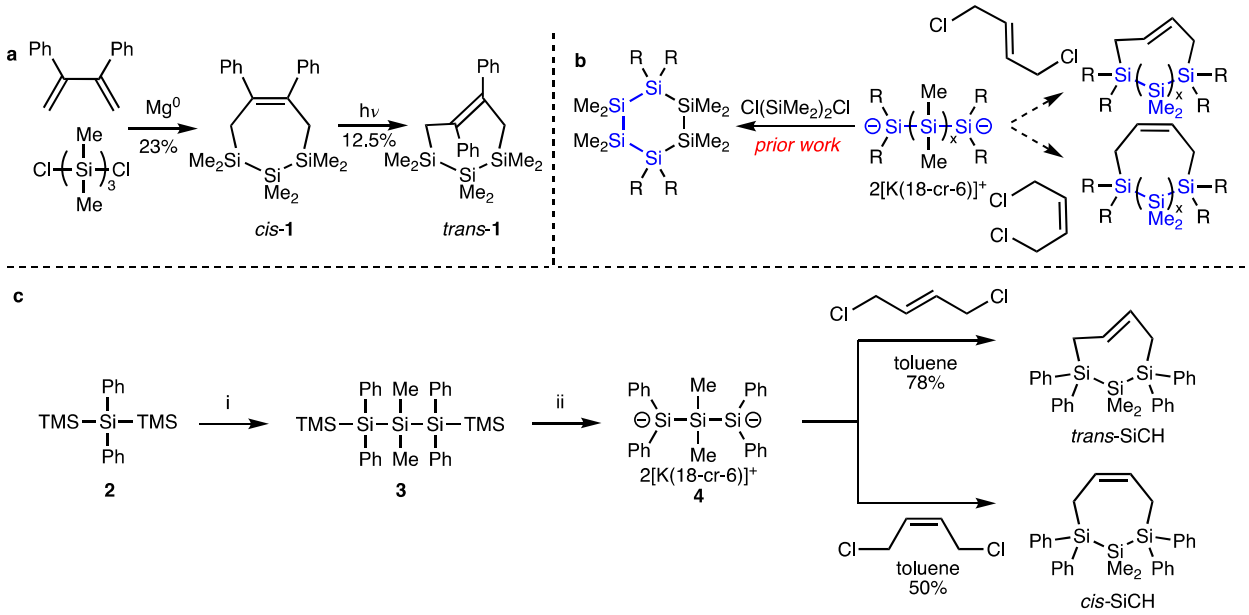

Scheme 1. a) Ando synthesis of *cis*- and *trans*-**1**. b) α,ω-Dipotassiooligosilyl dianions for silacycloalkene synthesis. c) Synthesis of isomeric *trans*- and *cis*-SiCH. i) KO*t*-Bu, THF, rt, 2h; Cl_2SiMe_2, -78 ºC, 16 h, 64% yield; ii) KO*t*-Bu, 18-cr-6, Et_2O, rt, 16 h, 71% yield.

Recognizing the need for geometrically pure cycloalkenes, we hypothesized that isomeric silacycloheptenes could be obtained by reaction of isomeric 1,4-dichlorobutenes with the same oligosilyl dianion (Scheme 1b). We and others have previously described the synthesis of α,ω-dipotassiooligosilyl dianions (x = 2-3)[45] via end-selective desilylation[46] and have shown that these dianions are suitable for gram-scale synthesis of cyclohexasilanes[47–51] and cyclosilaboranes.[52,53] To make the 7-membered ring, we synthesized novel dianion **4** by displacement of terminal trimethylsilane groups with potassium tert-butoxide (Scheme 1c). An X-ray crystal structure of **4** (Figure 2) was consistent with crystal structures of higher disilanides[45] in which K^+ engaged in a cation-π interaction with a phenyl group rather than a contact ion pair with the silyl anion. In dilute toluene, coupling of **4** with either *trans*- or *cis*-1,4-dichlorobutene proceeded smoothly to provide

geometrically pure *trans*- and *cis*-SiCH (Figure S1). In other solvents, competitive oligomerization and/or dianion decomposition was observed. The SiCH isomers could be isolated by silica gel chromatography, although generally in lower yield (ca. 30%), which was hypothesized to result from the acid sensitivity of the allylic silane. Pure samples could instead be obtained by precipitation or crystallization (50-78% yield).

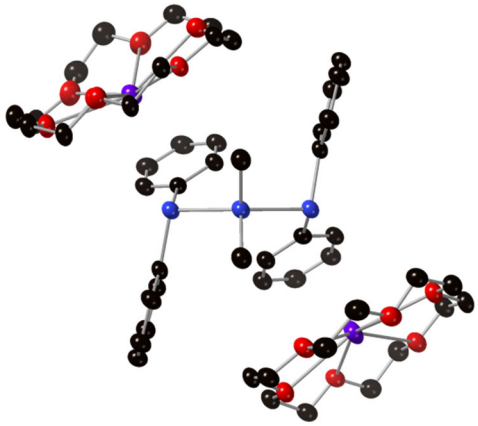

Figure 2. Displacement ellipsoid plot (50% probability level) of dianion **4** at 110(2) K. Hydrogens, coordinated THF solvent molecule, and disorder in 18-cr-6 omitted for clarity. Black = carbon, blue = silicon, red = oxygen, purple = potassium.

Single Crystal X-ray Crystallography. The molecular structures of the isomeric silacycloheptenes were determined by single crystal X-ray crystallography, which confirmed the isomer assignments. The conformation of *cis*-SiCH is boat-like, with three coplanar Si atoms and a central mirror plane of symmetry (Figure 3a), while *trans*-SiCH has a C2-axis of symmetry (Figure 3b). The symmetry of *trans*-SiCH is similar to Ando's *trans*-**1** and ^{1}H and ^{13}C NMR chemical shifts are also similar for the two strained cycloalkenes (Table S1).

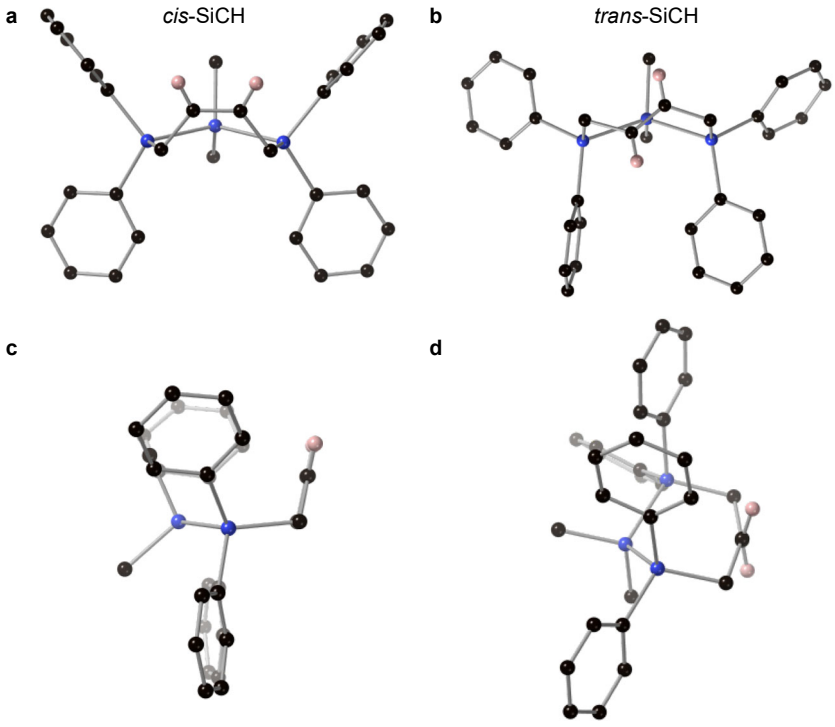

Figure 3. Displacement ellipsoid plots (50% probability level) of a) *cis*- and b) *trans*-SiCH at 110(2) K confirming geometric assignments. Newman projections along the olefinic C=C bond in c) *cis*-SiCH and d) *trans*-Si-CH consistent with low- and high-strain cycloalkenes. Hydrogens (except for olefinic protons) and disorder (occurring only for *trans*-SiCH) are omitted for clarity. Black = carbon, blue = silicon, pink = hydrogen.

Ring strain calculations (M06/def2-TZVPP-CPCM(DCM)//B3LYP-D4/def2-SVP) predicted that *cis*-SiCH would be lower strain (1.6 kcal mol^{-1}), while *trans*-SiCH would be higher strain (9.7 kcal mol^{-1}) (Figure S8). These calculations are consistent with the crystal structures. In low-strain *cis*-SiCH, the alkene is planar, as indicated by a planar C=C bond (Figure 3c). In contrast, the *trans*-SiCH olefin is twisted from planarity (Figure 3d). Table 1 summarizes some key structural parameters of the olefin in *cis*- and *trans*-SiCH, such as the torsion angle θ ($\angle C27-C28-C29-C30$), which is approximately 0 for *cis*-SiCH (planar olefin) and significantly less than 180° for *trans*-SiCH (twisted olefin). The bond lengths and angles are otherwise consistent with a double bond in both isomers. The C28–C29 bond distance in both isomers is basically the same (1.32 vs 1.33 Å) and consistent with a typical C=C bond (1.34 Å). The bond angles are close to 120°.

Table 1. Selected olefinic structural parameters.

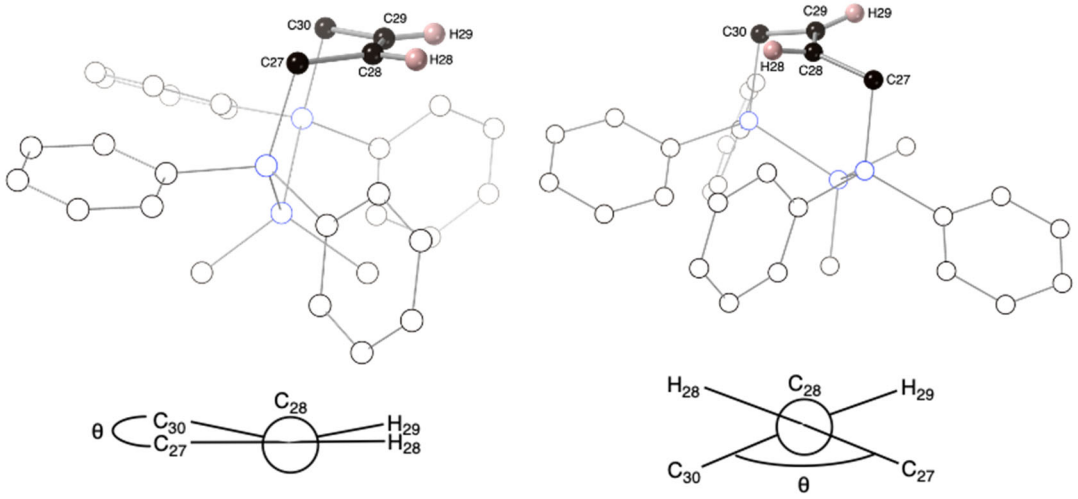

Structural Parameter	Abbreviation	*cis*-SiCH	*trans*-SiCH
$\angle C27-C28-C29-C30$	θ	-0.3(9)°	149.9(2)°
$\angle H28-C28-C29-C30$	n/a	179.6º	–30.0º
Distance C28=C29	n/a	1.329(6) Å	1.320(4) Å
$\angle C27-C28-C29$	n/a	126.1(5)°	122.4(3)°

Thermal Stability. Due to the rapid room temperature Z→E isomerization of *trans*-CH, we investigated the stability of *trans*-SiCH to storage at room temperature. Over the course of 8 days, a benzene-d_6 solution of *trans*-SiCH stored in the dark showed no appearance of signals corresponding to *cis*-SiCH by ^{1}H NMR spectroscopy (Figure S2). This is consistent with Ando's report that *trans*-**1** does not isomerize at room temperature.[13]

The rapid thermal isomerization of *trans*-CH to *cis*-CH has been attributed to a bimolecular mechanism involving a 1,4-biradical intermediate, as calculations of unimolecular isomerization via a 1,2-biradical suggested that *trans*-CH should be stable at room temperature.[6] Similarly, DFT

simulations estimated a barrier around 50 kcal mol^{-1} to thermal isomerization of *trans*-SiCH via a 1,2-biradical, based on a dihedral scan of the carbon/carbon double bond (Figures S8-S9). Furthermore, we also investigated a thermal isomerization of *trans*-SiCH through a bimolecular mechanism. While the dimerization towards the formation of 1,4-biradical of *trans*-CH was slightly exergonic (ΔG = -1.1 kcal/mol), the dimerization of *trans*-SiCH, which is significantly less strained than *trans*-CH, was highly endergonic (ΔG = 30.0 kcal/mol) making isomerization through a bimolecular mechanism kinetically inaccessible.

Ring-Opening Metathesis Polymerization. Using the second-generation Grubbs catalyst (G2, Figure 4a), we attempted ROMP of *cis*-SiCH. The comparatively poor solubility of *cis*-SiCH at room temperature required high dilution ([*cis*-SiCH]$_0$ = 0.10 M in CH_2Cl_2) not usually effective for entropy-driven ROMP of low strain monomers[2] and ROMP was not observed (Table 2). Starting material was recovered (Figure 4b), which indicated that the Si–Si bonds of SiCH were stable to G2, a conclusion supported by also evaluating *cis*-CO ROMP in the presence of a tetrasilane additive (Figure S3).

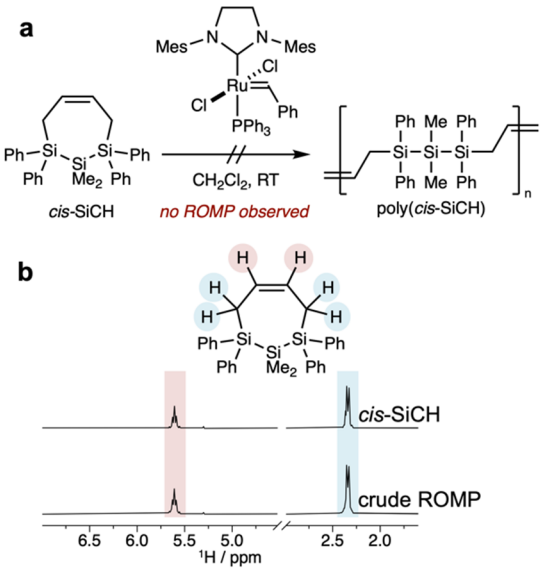

Figure 4. a) *cis*-SiCH ROMP with Grubbs 2nd generation catalyst (G2) did not provide poly(*cis*-SiCH). b) Superimposed cropped ^{1}H NMR spectra of *cis*-SiH (top) and after 24 hours of reaction with G2 (bottom) showing unreacted monomer.

In contrast, under similar conditions (Scheme 2a), within 15 minutes *trans*-SiCH underwent ROMP to provide a glassy white polymer (Scheme 2b). Size exclusion chromatography (SEC, Figure 5 and Table 2, entry 4) showed a high molar mass (M_n = 62,700 g mol^{-1}), relatively disperse polymer (M_w/M_n = 3.44). Variation of the ratio of monomer to initiator had little effect on M_n but reduced M_w/M_n from ca. 3.5 to 2.2 (entries 5-6). These data suggest that *trans*-SiCH ROMP is not living under the conditions investigated. While the comparable results were obtained with G2 and G1 (compare entries 4 and 7), the addition of excess PPh_3 (60 equiv.), known to result in better control in ROMP of *trans*-CO[10] and other cycloalkenes,[54] dramatically reduced M_n to 7370 g mol^{-1} while also providing narrower dispersity (3.50 vs. 1.38, entry 8).

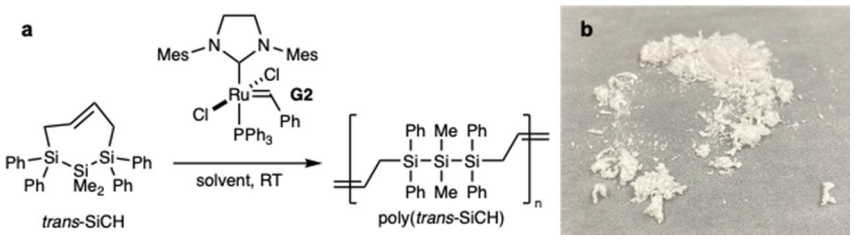

Scheme 2. a) ROMP of *trans*-SiCH (see Table 2 for conditions) and b) photograph of glassy white poly(*trans*-SiCH).

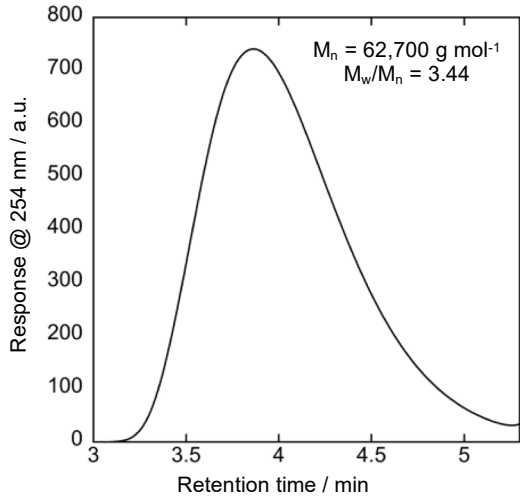

Figure 5. Size exclusion chromatogram ([poly(*trans*-SiCH)] = 1 mg mL^{-1}, THF, RT) relative to polystyrene standards.

Table 2. ROMP of *cis*- and *trans*-SiCH.

Entry	Monomer	Initiator	$[M]_0/[I]$	Time	Yield (%)	M_n (kg mol^{-1})[a]	M_w/M_n [a]
1	*cis*-SiCH	G2	1000/1	5 h	0	n.d.	n.d.
2	*cis*-SiCH	G2	1200/1	5 h	0	n.d.	n.d.
3	*cis*-SiCH	G2	1200/1	24 h	0	n.d.	n.d.
Entry	**Monomer**	**Initiator**	**$[M]_0/[I]$**	**Time**	**Yield (%)**	**M_n (kg mol^{-1})[a]**	**M_w/M_n [a]**
4	*trans*-SiCH	G2	500/1	1 h	36	62.6	3.50
5	*trans*-SiCH	G2	1000/1	1 h	70	51.5	2.43
6	*trans*-SiCH	G2	100/1	1 h	33	39.0	3.02
7	*trans*-SiCH	G1	500/1	1 h	64	62.3	3.56
8	*trans*-SiCH [b]	G1	500/1	1 h	4.0	7.37	1.38

ROMP of *cis*-SICH and *trans*-SiCH were performed at room temperature with solutions of 0.1M and 2.4M in DCM respectively. [a] Determined by size exclusion chromatography relative to polystyrene standards at 254 nm (THF, [poly(*trans*-SiCH)] = 1 mg mL^{-1}, 40 °C, 0.35 mL min^{-1}, 10 µL injection). [b] With 60 equiv. PPh_3 relative to **G1**.

To better understand reactivity differences between *trans*- and *cis*-SiCH, we carried out DFT calculations of ring-opening metathesis with a simplified permethyloligosilane model substrate.

The rate-determining step for both monomers was identified as the retro [2+2]-cycloaddition leading to ring-opening (e.g., **IV**→**V**). This step was kinetically accessible (i.e., activation energies of 10.6 and 18.6 kcal mol^{-1}, respectively) for both monomers, relative to the phosphine ligand bound intermediate (Figure 6). However, while ring-opening metathesis is exergonic by 1.5 kcal mol^{-1} for *trans*-SiCH (**V-trans** relative to **III-trans** and free ***trans*-SiCH**), it is endergonic for *cis*-SiCH by 6.0 kcal mol^{-1} (**V-cis** relative to **III-cis** and free ***cis*-SiCH**), which is consistent with their respective ring strain and reactivity. The kinetically accessible barriers to *cis*-SiCH ROMP suggest that polymerization of *cis*-SiCH should be possible, if an appropriate solvent and concentration were identified for entropy-driven ROMP.

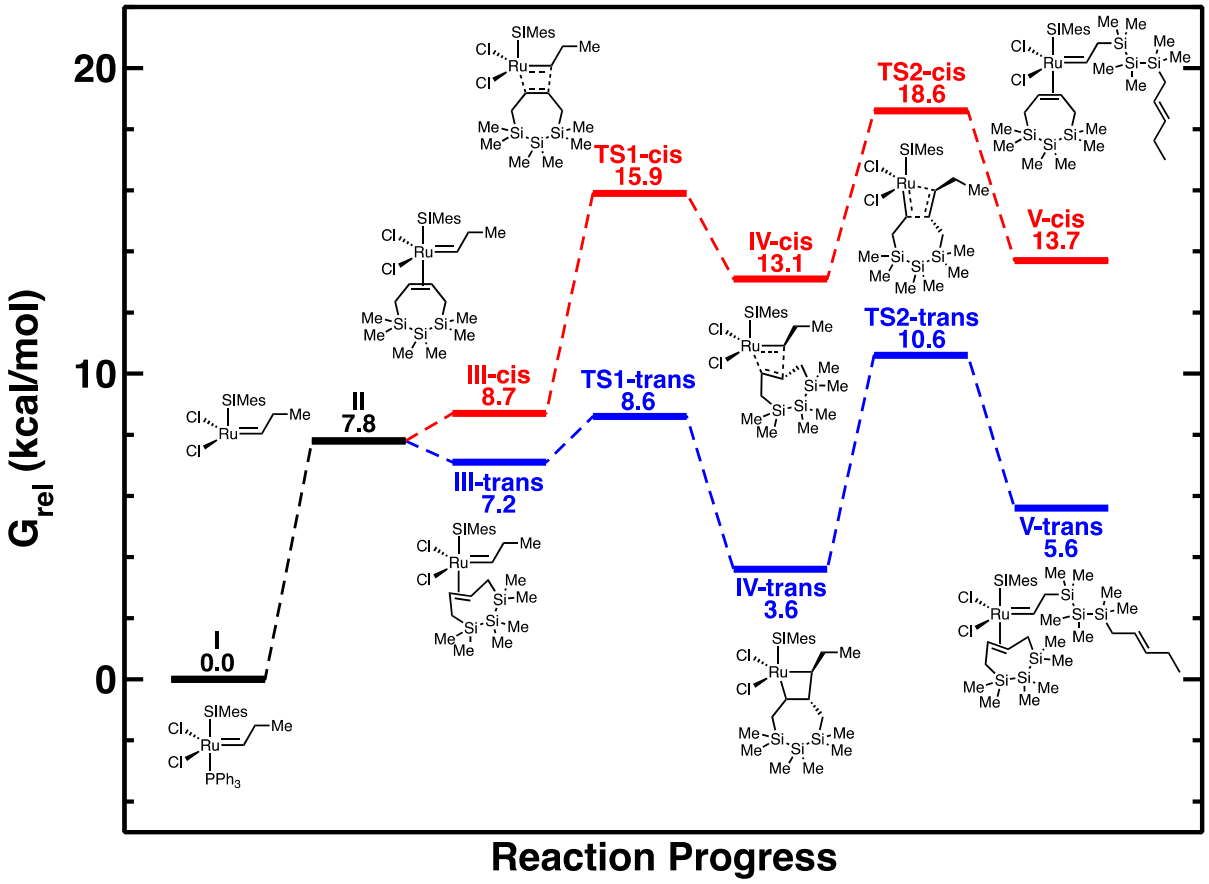

Figure 6. Potential energy surface (in kcal/mol) calculated at the M06/def2-TZVPP-CPCM(DCM)// B3LYP-D4/def2-SVP level of theory for ROMP initiation. All energies refer to Gibbs free energies and are relative to **I** and two SiCH cycles. The *trans*-SiCH initiation is shown in blue and the *cis*-SiCH initiation is shown in blue, with common PPh_3 ligated Ru and free Ru catalyst shown in black.

Poly(*trans*-SiCH) Characterization. Poly(*trans*-SiCH) was fully characterized by ^{1}H, ^{13}C, and ^{29}Si NMR spectroscopy (Figure 7). Resonances consistent with the expected aromatic, vinylic, allylic, and methylsilane peaks were observed (Figure 7a). The ^{29}Si distortionless enhancement by polarization transfer (DEPT)[55] spectrum showed resonances consistent with both methylsilanes and phenylsilanes (Figure 7b). The assignment of the δ –45 resonances to the $SiMe_2$ moiety was based on the greater signal intensity expected for methylsilanes compared to phenylsilanes in a ^{1}H→^{29}Si polarization transfer NMR experiment; the methylsilane has six protons two bonds away

($^2J_{1H\text{-}29Si}$ = 7-10 Hz), while the phenylsilane has 4 protons three bonds away. The relative chemical shifts are also consistent with internal and end group resonances in oligosilanes.[56]

The ^{1}H NMR spectrum indicated that ROMP was not stereoselective, as expected for G2, as resonances consistent with the presence of both *trans*- and *cis*-alkenes (ca. 1.5:1) were observed at δ 5.25 and 5.16 (Figure 7a). The major isomer was assigned to the *trans*-alkene based on the relatively downfield chemical shift of *trans*-SiCH compared to *cis*-SiCH. This is consistent with ROMP of *cis*-CH using the same catalyst, which afforded a polymer containing predominantly the *trans*-olefin (ca. 5:1).[2] The ^{13}C NMR spectrum also showed two peaks consistent with two distinct vinylic environments (Figure 7c). The ^{1}H-^{13}C HSQC (heteronuclear single quantum coherence) spectrum (Figure 7d) showed that the vinylic protons coupled to distinct vinylic carbons. The IR spectrum also showed resonances consistent with both cis and *trans* C=C stretching frequencies[57] in the 1660–1630 cm^{-1} region (Figure S4).

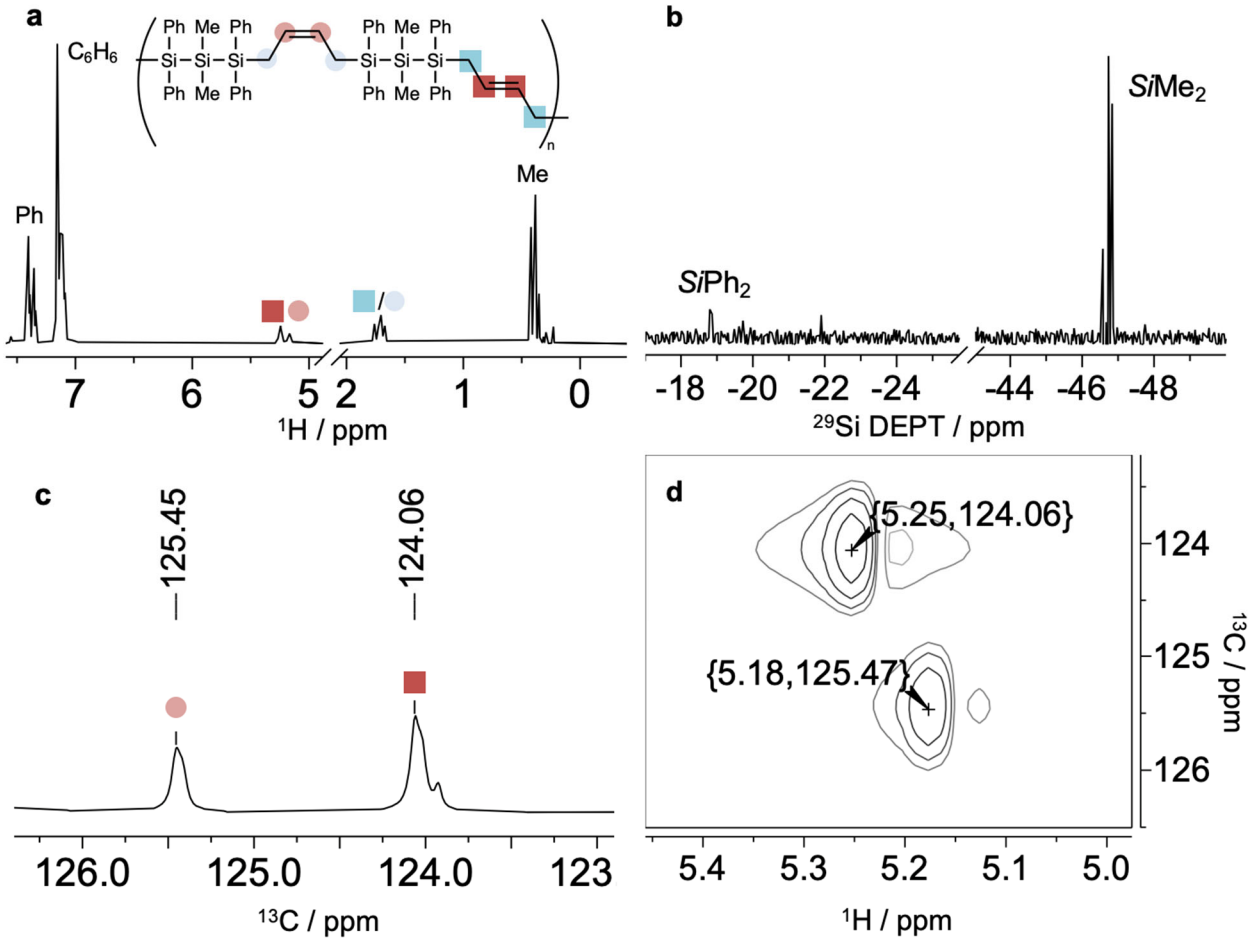

Figure 7. a) Cropped ^{1}H NMR spectrum (benzene-d_6, 600 MHz) of poly(*trans*-SiCH) showing evidence of aromatic, vinylic, allylic, and methysilane resonances. b) ^{29}Si NMR spectrum of poly(*trans*-SiCH). c) Cropped ^{13}C NMR spectrum (benzene-d_6, 600 MHz) of poly(*trans*-SiCH) focusing on vinylic carbons assigned to *cis*- and *trans*-olefins. d) ^{1}H-^{13}C HSQC confirms one-bond correlation between signals assigned to olefinic resonances.

Solution-state UV-vis spectra were collected for both *cis*- and *trans*-SiCH, which were identical in λ_{max} of ca. 250 nm (Figure S5). This is consistent with prior reports of aryl-substituted trisilanes.[44] A similar absorption band was found for poly(*trans*-SiCH), suggesting retention of the trisilane chromophore after ring-opening metathesis polymerization (Figure S6).

The thermal properties of poly(*trans*-SiCH) were determined by differential scanning calorimetry (DSC) and thermogravimetric analysis (TGA). The pyrolysis, under inert atmosphere, of polysilanes and polycarbosilanes to silicon carbide is well-known,[58,59] with polysilanes typically beginning thermal decomposition around 200-250 °C.[60] To identify the upper limit of poly(trans-SiCH) thermal stability, we obtained TGA data under an inert nitrogen atmosphere. The maximum mass loss was observed at 355 °C, with the onset of decomposition ca. 300 °C (Figure 8a). This is a lower level of thermal stability than poly(*cis*-CO), which begins to degrade >400 °C,[61] consistent with retention of the trisilane in poly(*trans*-SiCH).

We also investigated the thermal properties below the decomposition temperature, as the elasticity of polyoctenamers depends on polymer stereoregularity: predominantly *cis*-alkenes results in a viscoelastic material, while predominantly *trans*-alkenes are semicrystalline.[62] Both exhibit a glass transition temperature (T_g) ca. –80 °C. Our poly(*trans*-SiCH), synthesized as a ca. 1.5:1 mixture of olefinic isomers, exhibited a T_g of 39.7 °C (Figure 8b), significantly higher than polyCO, which was attributed to the stiffening effect of the four phenyl side chains.

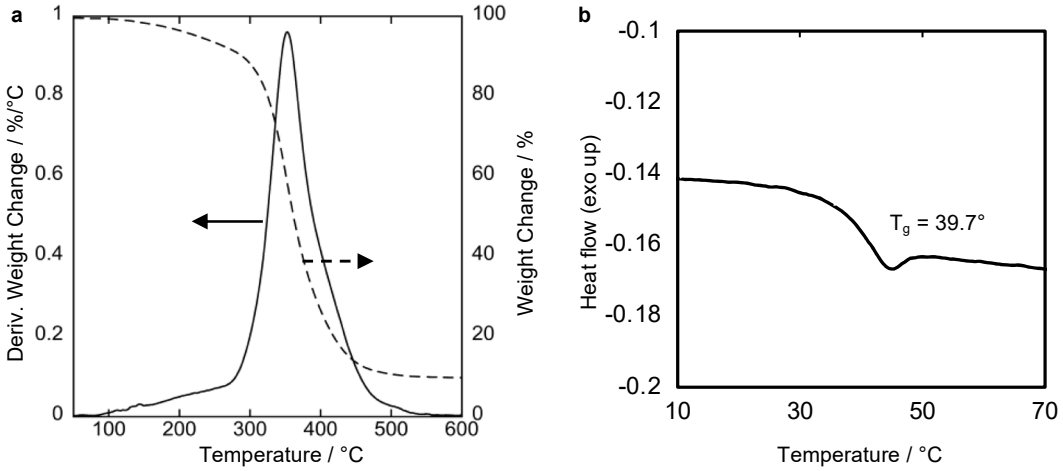

Figure 8. a) Thermal decomposition of poly(*trans*-SiCH) under a nitrogen atmosphere. b) Glass transition temperature (T_g) of poly(*trans*-SiCH) obtained by differential scanning calorimetry. Second heating cycle shown. See Figure S7 for full image. Heating rate: 20 °C min^{-1}, cooling rate: 10 °C min$^{-1.}$

Single-Molecule Force Spectroscopy.

To compare the force-coupled behavior of silicon-rich polymers with all-carbon analogues, we carried out both computational modeling and experimental studies. We optimized under external force geometries of molecular fragments **5-7** (Figure 9) that were designed to mimic the constitutional repeat units of poly(SiCH) and poly(CO), as well as *cis* and *trans* polybutadiene. Here, we increased the external force in increments of 50 pN over the range of 0-3 nN on the internal sp^2 carbons (Figure 9). The distances between these two sp^2 carbons were obtained at each external force and were normalized to their length of force-free optimized structures (i.e., L/L_0). The **5**, **6** and *trans*-**7** fragments show linear extension with increasing force, whereas the *cis*-**7** fragment has a significantly larger extension in the low-force region, which can be attributed to the poor initial alignment of the central cis bond with the force vector at low forces due to low-energy dihedral rotations (Figure S12). Therefore, we chose to obtain our linear fit over all four structures in the 1.5-3.0 nN force regions to estimate elasticity of these fragments as the slope of external force vs. normalized extension. These calculations suggested that Si-rich materials are distorted more readily compared to their all-carbon analogues (Figure S13) and would exhibit substantially lower elasticity. The SiCH monomer **5** has an elasticity (1.8×10^4 pN per unit L_0) that

is half the value for the all-carbon **6** (3.6×10^4 pN per unit L_0). For **7**, the elasticity is still higher than silane **5**, for both the trans fragment (3.6×10^4 pN per unit L_0) and cis fragment (2.0×10^4 pN per unit L_0). Accounting for the 63% *cis* and 37% *trans* composition of PB, we estimate the elasticity for this composition (2.5×10^4 pN per unit L_0) to still be 40% higher than that for SiCH.

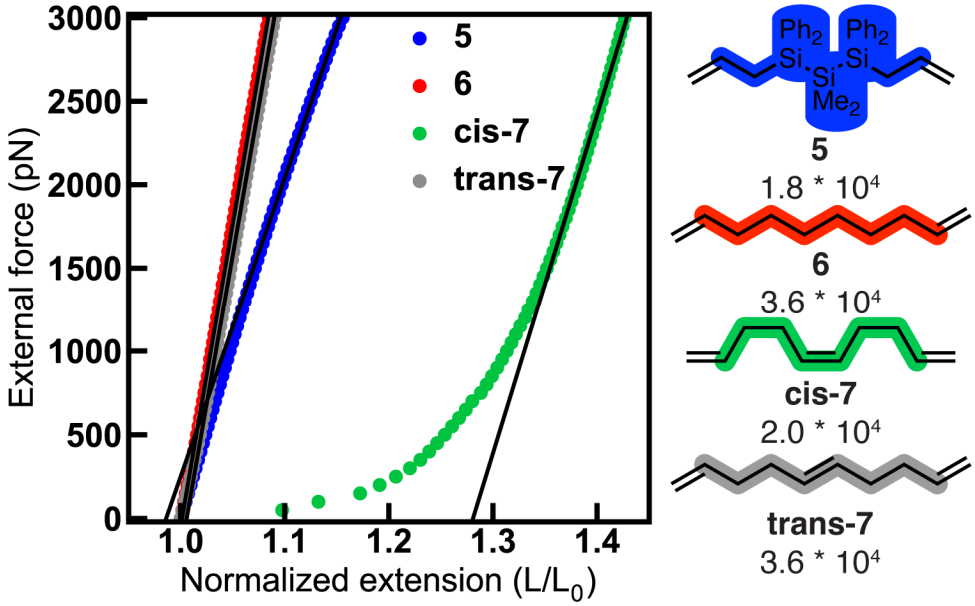

Figure 9. Relative force-coupled extension of fragments **5–7** calculated with external force explicitly included (EFEI) method. The external force was applied to the endpoints of the highlighted fragments in the structures shown at right, and distances between these two atoms were normalized to their length of force-free optimized structures (i.e., L/L_0). Structures shown at right are annotated with their elasticity annotated in units of pN per unit L_0.

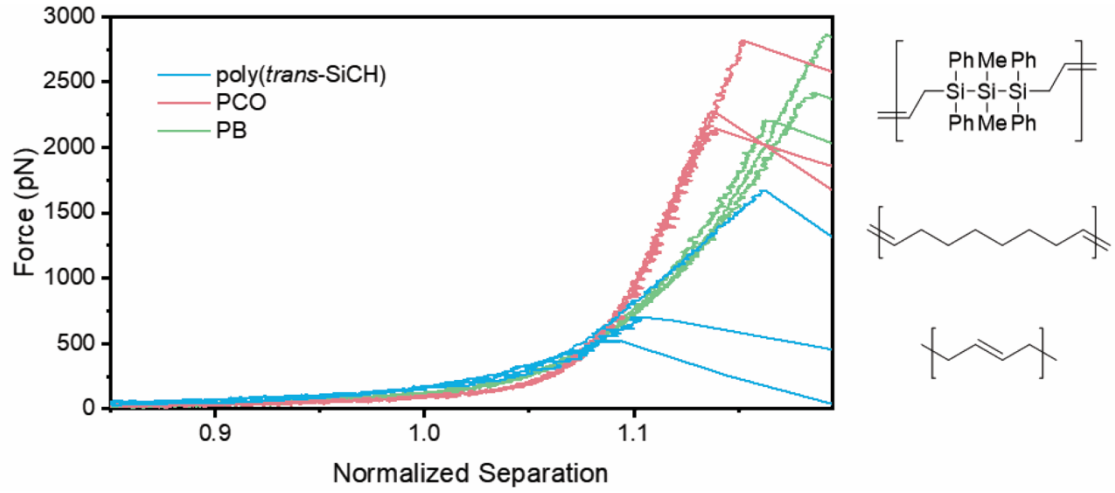

Figure 10. Representative single-molecule force-extension curves of poly(trans-SiCH, cis: trans 1:1.41), polycyclooctene (PCO, cis:trans 1:3.54) and polybutadiene (PB, cis:trans 1.70:1) normalized at 500 pN.

We performed single molecule force spectroscopy (SMFS) on poly(*trans*-SiCH) and the carbon-based analogs polycyclooctene (PCO) and polybutadiene (PB). Prior work has shown that side chains have little impact on chain flexibility and therefore the aromatic side chains of poly(*trans*-SiCH) could be neglected in selecting control polymers.[22] Obtained force-extension curves are

shown in Figure 10. The curves were fit with a modified freely-jointed chain model to obtain a nominal contour length L_0, and the extensional behavior beyond L_0 differs across the series. In particular, the slope of poly(*trans*-SiCH) is lower than that of both of PCO and PB, consistent with the calculations (Figure 9). To quantify the impact of the Si on elasticity, we compare the slope of each force-extension curve from 1000 pN to the point at which the polymer detaches (Table 3). Even at just three Si atoms per repeat, the elasticity of poly(*trans*-SiCH) is 1.4×10^4 pN per unit L_0, significantly lower than 3.5×10^4 pN and 2.4×10^4 pN, respectively, for PCO and PB. Looking ahead, access to Si-rich polymers with enhanced compliance offers opportunities to probe the contributions of strand elasticity to the mechanical properties of polymer networks, including fracture.[63]

Table 3. slopes of the high-force region (F > 1000 pN) of the force-extension curves

	Elasticity (pN×10^4 per unit L_0)
poly(trans-SiCH)	1.4
PCO	3.5 ± 0.1
PB	2.4 ± 0.2

Conclusions

Herein, we report the synthesis of a new class of silicon-rich polymer derived from ring-opening metathesis polymerization (ROMP) of a strained *trans*-silacycloheptene. Geometrically pure isomers of the silacycloheptene were synthesized by a novel approach, the alkylation of an α,ω-dipotassiodisilanide. Structure assignments for each isomeric monomer were confirmed by X-ray crystallography, which also provided structural signatures of low- and high-ring strain e.g., a twisted olefin. The higher-strain *trans*-SiCH underwent rapid ROMP to provide a glassy organometallic polymer, which was fully characterized by ^{1}H, ^{13}C, and ^{29}Si NMR spectroscopy as well as IR and UV-vis spectroscopy and thermal characterization (e.g., TGA and DSC). Insights into the room-temperature stability to isomerization of *trans*-SiCH were obtained by quantum chemical calculations, which suggested a high thermal barrier to either unimolecular formation of a 1,2-biradical or bimolecular formation of a 1,4-biradical.

We hypothesized that Si incorporation into the backbone could lead to distinctive force-coupled extensional behavior in single polymer chains. Computational models predicted that incorporating a trisilane in place of three methylenes in polycycloheptene would result in a more stretchable backbone than comparable all C–C backbones. Force-extension curves from SMFS showed that the extended poly(*trans*-SiCH) has a smaller spring constant compared to two carbon-based analogs, polycyclooctene and polybutadiene. Our results point to the possibility of employing Si-rich polymers to prove the contribution of strand elasticity to the mechanical properties of bulk polymer networks.

CCDC Deposition

2223766-2223767, 2234184

Supporting Information

The Supporting Information is available free of charge at https://pubs.acs.org/doi/10.1021/jacs.2c10462.

Synthesis procedures and analytical; experimental methods; additional experimental data; supporting discussion and calculations (PDF)

Acknowledgements

This work was supported by the NSF Center for the Chemistry of Molecularly Optimized Networks (MONET; Award CHE-2116298). This work used Expanse at San Diego Supercomputing Center

through allocation CHE-140073 from the Advanced Cyberinfrastructure Coordination Ecosystem: Services and Support (ACCESS) program, which is supported by National Science Foundation Grants #2138259, #2138286, #2138307, #2137603, and #2138296. E. G. A. thanks Johns Hopkins University for a Provost's Undergraduate Research Award. We thank Dr. Ananya Majumdar (JHU Biophysical NMR Center) for assistance with high field NMR spectroscopy, Dr. V. Sara Thoi (JHU) and Mr. Fan Fang (JHU) for assistance with TGA, and Dr. Eric A. Marro for helpful discussion of dianion synthesis.

References

(1) Neary, W. J.; Kennemur, J. G. Polypentenamer Renaissance: Challenges and Opportunities. *ACS Macro Lett.* **2019**, *8* (1), 46–56.

(2) Hejl, A.; Scherman, O. A.; Grubbs, R. H. Ring-Opening Metathesis Polymerization of Functionalized Low-Strain Monomers with Ruthenium-Based Catalysts. *Macromolecules* **2005**, *38* (17), 7214–7218.

(3) Hlil, A. R.; Balogh, J.; Moncho, S.; Su, H.-L.; Tuba, R.; Brothers, E. N.; Al-Hashimi, M.; Bazzi, H. S. Ring Opening Metathesis Polymerization (ROMP) of Five- to Eight-Membered Cyclic Olefins: Computational, Thermodynamic, and Experimental Approach. *J. Polym. Sci. Part A Polym. Chem.* **2017**, *55* (18), 3137–3145.

(4) Pearce, A. K.; Foster, J. C.; O'Reilly, R. K. Recent Developments in Entropy driven Ring opening Metathesis Polymerization: Mechanistic Considerations, Unique Functionality, and Sequence Control. *J. Polym. Sci. Part A Polym. Chem.* **2019**, *57* (15), 1621–1634.

(5) Barrows, S. E.; Eberlein, T. H. Cis and Trans Isomers of Cycloalkenes. *J. Chem. Educ.* **2005**, *82* (9), 1334–1339.

(6) Squillacote, M. E.; DeFellipis, J.; Shu, Q. How Stable Is Trans-Cycloheptene? *J. Am. Chem. Soc.* **2005**, *127* (45), 15983–15988.

(7) Wallraff, G. M.; Michl, J.; Boyd, R. H. Conformational Mobility in the Trans-Cycloheptene-Copper(I) Triflate Complex. *J. Am. Chem. Soc.* **1983**, *105* (14), 4550–4555.

(8) Hoffmann, R.; Inoue, Y. Trapped Optically Active (E)-Cycloheptene Generated by Enantiodifferentiating Z-E Photoisomerization of Cycloheptene Sensitized by Chiral Aromatic Esters. *J. Am. Chem. Soc.* **1999**, *121* (46), 10702–10710.

(9) Neveselý, T.; Wienhold, M.; Molloy, J. J.; Gilmour, R. Advances in the e → Z Isomerization of Alkenes Using Small Molecule Photocatalysts. *Chem. Rev.* **2022**, *122* (2), 2650–2694.

(10) Walker, R.; Conrad, R. M.; Grubbs, R. H. The Living ROMP of Trans-Cyclooctene. *Macromolecules* **2009**, *42* (3), 599–605.

(11) Sathe, D.; Zhou, J.; Chen, H.; Su, H. W.; Xie, W.; Hsu, T. G.; Schrage, B. R.; Smith, T.; Ziegler, C. J.; Wang, J. Olefin Metathesis-Based Chemically Recyclable Polymers Enabled by Fused-Ring Monomers. *Nat. Chem.* **2021**, *13* (8), 743–750.

(12) Chen, H.; Shi, Z.; Hsu, T.; Wang, J. Overcoming the Low Driving Force in Forming Depolymerizable Polymers through Monomer Isomerization. *Angew. Chemie Int. Ed.* **2021**, *60* (48), 25493–25498.

(13) Shimizu, T.; Shimizu, K.; Ando, W. Synthesis, Structure, and Stabilities of Trans-1,2-Diphenyl-4,4,5,5,6,6-Hexamethyl-4,5,6-Trisila-Cycloheptene. *J. Am. Chem. Soc.* **1991**, *113* (1), 354–355.

(14) Sanzone, J. R.; Woerpel, K. A. High Reactivity of Strained Seven-Membered-Ring *Trans* -Alkenes. *Angew. Chemie Int. Ed.* **2016**, *55* (2), 790–793.

(15) Fang, Y.; Zhang, H.; Huang, Z.; Scinto, S. L.; Yang, J. C.; Am Ende, C. W.; Dmitrenko, O.; Johnson, D. S.; Fox, J. M. Photochemical Syntheses, Transformations, and Bioorthogonal Chemistry of: Trans -Cycloheptene and Sila Trans -Cycloheptene Ag(i) Complexes. *Chem. Sci.* **2018**, *9* (7), 1953–1963.

(16) Krebs, A.; Pforr, K.-I.; Raffay, W.; Thölke, B.; König, W. A.; Hardt, I.; Boese, R. A Stable Hetero-Trans-Cyclopentene. *Angew. Chemie Int. Ed. English* **1997**, *36* (12), 159–160.

(17) Michl, J.; West, R. Conformations of Linear Chains. Systematics and Suggestions for Nomenclature. *Acc. Chem. Res.* **2000**, *33* (12), 821–823.

(18) Albinsson, B.; Teramae, H.; Downing, J. W.; Michl, J. Conformers of Saturated Chains: Matrix Isolation, Structure, IR and UV Spectra of *n* -Si_4 Me_{10}. *Chem. - A Eur. J.* **1996**, *2* (5), 529–538.

(19) Marszalek, P. E.; Oberhauser, A. F.; Pang, Y. P.; Fernandez, J. M. Polysaccharide Elasticity Governed by Chair-Boat Transitions of the Glucopyranose Ring. *Nature* **1998**, *396* (6712), 661–664.

(20) Binnig, G.; Quate, C. F.; Gerber, C. Atomic Force Microscope. *Phys. Rev. Lett.* **1986**, *56* (9), 930–933.

(21) Evans, E. A.; Ritchie, K. Strength of a Weak Bond Connecting Flexible Polymer Chains. *Biophys. J.* **1999**, *76* (5), 2439–2447.

(22) Wang, K.; Pang, X.; Cui, S. Inherent Stretching Elasticity of a Single Polymer Chain with a Carbon-Carbon Backbone. *Langmuir* **2013**, *29* (13), 4315–4319.

(23) Luo, Z.; Zhang, A.; Chen, Y.; Shen, Z.; Cui, S. How Big Is Big Enough? Effect of Length and Shape of Side Chains on the Single-Chain Enthalpic Elasticity of a Macromolecule. *Macromolecules* **2016**, *49* (9), 3559–3565.

(24) Li, H.; Zhang, W.; Xu, W.; Zhang, X. Hydrogen Bonding Governs the Elastic Properties of Poly(Vinyl Alcohol) in Water: Single-Molecule Force Spectroscopic Studies of PVA by AFM. *Macromolecules* **2000**, *33* (2), 465–469.

(25) Zhang, X.; Liu, C.; Wang, Z. Force Spectroscopy of Polymers: Studying on Intramolecular and Intermolecular Interactions in Single Molecular Level. *Polymer*. Elsevier BV July 28, 2008, pp 3353–3361.

(26) Song, Y.; Ma, Z.; Yang, P.; Zhang, X.; Lyu, X.; Jiang, K.; Zhang, W. Single-Molecule Force Spectroscopy Study on Force-Induced Melting in Polymer Single Crystals: The Chain Conformation Matters. *Macromolecules* **2019**, *52* (3), 1327–1333.

(27) Tilley, T. D. The Coordination Polymerization of Silanes to Polysilanes by a “σ-Bond Metathesis” Mechanism. Implications for Linear Chain Growth. *Acc. Chem. Res.* **1993**, *26* (1), 22–29.

(28) Jones, R. G.; Budnik, U.; Holder, S. J.; Wong, W. K. C. Reappraisal of the Origins of the Polymodal Molecular Mass Distributions in the Formation of Poly(Methylphenylsilylene) by the Wurtz Reductive-Coupling Reaction. *Macromolecules* **1996**, *29* (25), 8036–8046.

(29) Klausen, R. S.; Ballestero-Martínez, E. Organosilicon and Related Group 14 Polymers. In *Comprehensive Organometallic Chemistry IV*; Parkin, G., Meyer, K., O’Hare, D., Eds.; Elsevier, 2022; pp 135–165.

(30) McQuade, J.; Serrano, M. I.; Jäkle, F. Main Group Functionalized Polymers through Ring-Opening Metathesis Polymerization (ROMP). *Polymer (Guildf).* **2022**, *246*, 124739.

(31) Brzezinska, K. R.; Schitter, R.; Wagener, K. B. Carbosilane/Carbosiloxane-Based ADMET Homopolymers and Copolymers Possessing Latent Reactivity. *J. Polym. Sci. Part A Polym. Chem.* **2000**, *38* (9), 1544–1550.

(32) Cushman, K.; Keith, A.; Tanaka, J.; Sheiko, S. S.; You, W. Investigating the Stress-Strain Behavior in Ring-Opening Metathesis Polymerization-Based Brush Elastomers. *Macromolecules* **2021**, *54* (18), 8365–8371.

(33) Johnson, A. M.; Husted, K. E. L.; Kilgallon, L. J.; Johnson, J. A. Orthogonally Deconstructable and Depolymerizable Polysilylethers via Entropy-Driven Ring-Opening Metathesis Polymerization. *Chem. Commun.* **2022**, *58* (61), 8496–8499.

(34) Shieh, P.; Zhang, W.; Husted, K. E. L.; Kristufek, S. L.; Xiong, B.; Lundberg, D. J.; Lem, J.; Veysset, D.; Sun, Y.; Nelson, K. A.; et al. Cleavable Comonomers Enable Degradable, Recyclable Thermoset Plastics. *Nature* **2020**, *583* (7817), 542–547.

(35) Husted, K. E. L.; Shieh, P.; Lundberg, D. J.; Kristufek, S. L.; Johnson, J. A. Molecularly Designed Additives for Chemically Deconstructable Thermosets without Compromised Thermomechanical Properties. *ACS Macro Lett.* **2021**, *10* (7), 805–810.

(36) Ratushnyy, M.; Zhukhovitskiy, A. V. Polymer Skeletal Editing via Anionic Brook Rearrangements. *J. Am. Chem. Soc.* **2021**, *143* (43), 17931–17936.

(37) Rosenberg, L. Exploiting Catalytic Dehydrogenative Coupling in the Synthesis and Study of Polysilanes. *Macromol. Symp.* **2003**, *196* (1), 347–353.

(38) Jiang, Q.; Gittens, A. F.; Wong, S.; Siegler, M. A.; Klausen, R. S. Highly Selective Addition of Cyclosilanes to Alkynes Enabling New Conjugated Materials. *Chem. Sci.* **2022**, *13* (25), 7587–7593.

(39) Mark, J. E. Silicon-Containing Polymers. In *Silicon-Based Polymer Science*; American Chemical Society, 1989; pp 47–68.

(40) Birot, M.; Pillot, J. P.; Dunoguès, J. Comprehensive Chemistry of Polycarbosilanes, Polysilazanes, and Polycarbosilazanes as Precursors of Ceramics. *Chem. Rev.* **1995**, *95* (5), 1443–1477.

(41) Miller, R. D.; Michl, J. Polysilane High Polymers. *Chem. Rev.* **1989**, *89* (6), 1359–1410.

(42) Barroso, G.; Li, Q.; Bordia, R. K.; Motz, G. Polymeric and Ceramic Silicon-Based Coatings-a Review. *J. Mater. Chem. A* **2019**, *7* (5), 1936–1963.

(43) Waldeck, D. H. Photoisomerization Dynamics of Stilbenes. *Chem. Rev.* **1991**, *91* (3), 415–436.

(44) Gilman, H.; Atwell, W. H.; Schwebke, G. L. Ultraviolet Properties of Compounds Containing the Silicon-Silicon Bond. *J. Organomet. Chem.* **1964**, *2* (4), 369–371.

(45) Marro, E. A.; Press, E. M.; Purkait, T. K.; Jimenez, D.; Siegler, M. A.; Klausen, R. S. Cooperative Noncovalent Interactions Induce Ion Pair Separation in Diphenylsilanides. *Chem. - A Eur. J.* **2017**, *23* (62), 15633–15637.

(46) Kayser, C.; Kickelbick, G.; Marschner, C. Simple Synthesis of Oligosilyl-α,ω-Dipotassium Compounds. *Angew. Chemie Int. Ed.* **2002**, *41* (6), 989–992.

(47) Press, E. M.; Marro, E. A.; Surampudi, S. K.; Siegler, M. A.; Tang, J. A.; Klausen, R. S. Synthesis of a Fragment of Crystalline Silicon: Poly(Cyclosilane). *Angew. Chemie Int. Ed.*

2017, *56* (2), 568–572.

(48) Marro, E. A.; Press, E. M.; Siegler, M. A.; Klausen, R. S. Directional Building Blocks Determine Linear and Cyclic Silicon Architectures. *J. Am. Chem. Soc.* **2018**, *140* (8), 5976–5986.

(49) Marro, E. A.; Klausen, R. S. Conjugated Polymers Inspired by Crystalline Silicon. *Chem. Mater.* **2019**, *31* (7), 2202–2211.

(50) Marro, E. A.; Folster, C. P.; Press, E. M.; Im, H.; Ferguson, J. T.; Siegler, M. A.; Klausen, R. S. Stereocontrolled Syntheses of Functionalized Cis- and Trans-Siladecalins. *J. Am. Chem. Soc.* **2019**, *141* (44), 17926–17936.

(51) Fischer, R.; Frank, D.; Gaderbauer, W.; Kayser, C.; Mechtler, C.; Baumgartner, J.; Marschner, C. α,ω-Oligosilyl Dianions and Their Application in the Synthesis of Homo- and Heterocyclosilanes. *Organometallics* **2003**, *22* (18), 3723–3731.

(52) Purkait, T. K.; Press, E. M.; Marro, E. A.; Siegler, M. A.; Klausen, R. S. Low-Energy Electronic Transition in SiB Rings. *Organometallics* **2019**, *38* (8), 1688–1698.

(53) Markov, J.; Fischer, R.; Wagner, H.; Noormofidi, N.; Baumgartner, J.; Marschner, C. Open, Cyclic, and Bicyclic Compounds of Double Silylated Phosphorus and Boron. *Dalt. Trans.* **2004**, *51* (14), 2166.

(54) Bielawski, C. W.; Grubbs, R. H. Increasing the Initiation Efficiency of Ruthenium-Based Ring-Opening Metathesis Initiators: Effect of Excess Phosphine. *Macromolecules* **2001**, *34* (26), 8838–8840.

(55) Blinka, T. A.; Helmer, B. J.; West, R. Polarization Transfer NMR Spectroscopy for Silicon-29: The INEPT and DEPT Techniques. *Adv. Organomet. Chem.* **1984**, *23* (C), 193–218.

(56) Gupta, R. R.; Lechner, M. D. *Chemical Shifts and Coupling Constants for Silicon-29*; 2008; Vol. 35F.

(57) Binder, J. L. The Infrared Spectra and Structures of Polybutadienes. *J. Polym. Sci. Part A Gen. Pap.* **1963**, *1* (1), 47–58.

(58) Yajima, S.; Hasegawa, Y.; Okamura, K.; Matsuzawa, T. Development of High Tensile Strength Silicon Carbide Fibre Using an Organosilicon Polymer Precursor. *Nature* **1978**, *273* (5663), 525–527.

(59) Birot, M.; Pillot, J. P.; Dunoguès, J. Comprehensive Chemistry of Polycarbosilanes, Polysilazanes, and Polycarbosilazanes as Precursors of Ceramics. *Chem. Rev.* **1995**, *95*, 1443–1477.

(60) Jiang, Q.; Wong, S.; Klausen, R. S. Effect of Polycyclosilane Microstructure on Thermal Properties. *Polym. Chem.* **2021**, *12* (33), 4785–4794.

(61) Alonso-Villanueva, J.; Cuevas, J. M.; Laza, J. M.; Vilas, J. L.; León, L. M. Synthesis of Poly(Cyclooctene) by Ring-Opening Metathesis Polymerization: Characterization and Shape Memory Properties. *J. Appl. Polym. Sci.* **2010**, *115* (4), 2440–2447.

(62) Rylski, A. K.; Cater, H. L.; Mason, K. S.; Allen, M. J.; Arrowood, A. J.; Freeman, B. D.; Sanoja, G. E.; Page, Z. A. Polymeric Multimaterials by Photochemical Patterning of Crystallinity. *Science (80-.).* **2022**, *378* (6616), 211–215.

(63) Wang, S.; Panyukov, S.; Rubinstein, M.; Craig, S. L. Quantitative Adjustment to the Molecular Energy Parameter in the Lake-Thomas Theory of Polymer Fracture Energy. *Macromolecules* **2019**, *52* (7), 2772–2777.

TOC Graphic

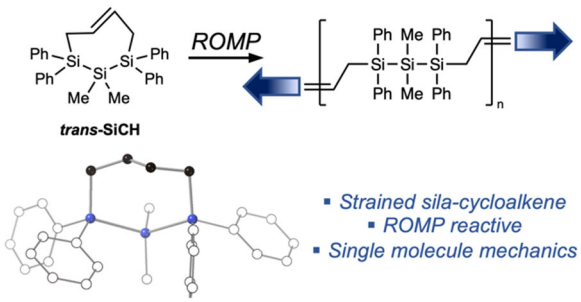
ROMP
trans-SiCH
▪ Strained sila-cycloalkene
▪ ROMP reactive
▪ Single molecule mechanics